# Improvement of Ground Slope Modification Factors for Cohesion and Friction Bearing Capacity Terms using Numerical Investigation of Square Footings

Yohannes Eshetu Ayalew
*Bahir Dar Institute of Technology, Bahir Dar University, Bahir Dar, Ethiopia*
Abraham Mineneh
*WSP Canada Inc., Calgary, Alberta, Canada*

ABSTRACT
Series of finite element numerical simulations were carried out using PLAXIS3D commercial software to study the effect of ground slopes on bearing capacity of square footings placed on ground surface without embedment. The numerical study was carried out for cohesionless soil in drained condition and cohesive soil in undrained condition. The series of simulations were conducted by varying the ground slope angle, setback distance of footing from slope crest, footing width and shear strength parameters of soil, which were soil friction angle for cohesionless soil and undrained cohesion for cohesive soil. The range of shear strength parameter values were selected to reflect the commonly encountered values in practice. For cohesionless soil, the maximum ground slope angle was limited to the soil friction angle; while for cohesive soil, slope stability analysis was conducted to determine the maximum slope angle for each chosen value of undrained cohesion. The simulation results indicate that the effect of ground slope on bearing capacity diminishes beyond a setback distance to footing width ratio of about 0.75 for undrained cohesive soil and 2 for drained cohesionless soil. This finding agrees with the semi-analytical approach by Bowles (1997) for footings near slope. However, Bowles' approach predicted ±30% of the measured bearing capacities from the numerical simulations. On the other hand, the ground modification factors suggested by Hansen (1970) and Vesic (1975) for the conventional bearing capacity equation can be applied only for the case of footings placed on slope crest. Thus, in this paper, improved ground modification factors are proposed for the cohesion term ($N_c$) and friction term ($N_\gamma$) of the conventional bearing capacity equation using the simulations data on cohesive soil and cohesionless soil, respectively.

RÉSUMÉ
Des séries de simulations numériques par éléments finis ont été effectuées à l'aide d'un logiciel commercial PLAXIS3D pour étudier l'effet des pentes du sol sur la capacité portante des semelles carrées placées sur la surface du sol sans intégration. L'étude numérique a été réalisée pour les sols sans cohésion dans des conditions drainées et les sols cohésifs dans un état non drainé. La série de simulations a été réalisée en faisant varier l'angle de pente du sol, la distance de retrait de la semelle par rapport à la crête de la pente, la largeur de la semelle et les paramètres de résistance au cisaillement du sol, qui étaient l'angle de frottement du sol pour un sol sans cohésion et la cohésion non tirée pour le sol cohésif. La marge des valeurs des paramètres de résistance au cisaillement a été choisie pour refléter les valeurs couramment rencontrées dans la pratique. Pour le sol sans cohésion, l'angle maximal de pente du sol était limité à l'angle de frottement du sol; tandis que pour un sol cohésif, une analyse de la stabilité des pentes a été effectuée pour déterminer l'angle de pente maximal pour chaque valeur choisie de cohésion non drainée. Les résultats de la simulation indiquent que l'effet de la pente du sol sur la capacité portante diminue au-delà d'un rapport distance de retrait à la largeur de la semelle d'environ 0,75 pour les sols cohésifs non drainés et de 2 pour les sols drainés sans cohésion. Cette constatation concorde avec l'approche semi-analytique de Bowles (1997) pour les semelles près de la pente. Cependant, l'approche de Bowles prévoyait ±30% des capacités portantes mesurées à partir des simulations numériques. D'autre part, les facteurs de modification du sol suggérés par Hansen (1970) et Vesic (1975) pour l'équation de la capacité portante conventionnelle ne peuvent être appliqués que pour le cas des semelles placées sur la crête de pente. Ainsi, dans le présent document, des facteurs améliorés de modification du sol sont proposés pour le terme de cohésion ($N_c$) et le terme de frottement ($N_\gamma$) de l'équation de la capacité portante conventionnelle en utilisant les données de simulation sur le sol cohésif et le sol sans cohésion, respectivement.

## 1 INTRODUCTION

The ultimate bearing capacity ($q_u$) of a foundation is the maximum load that can be supported by a foundation without causing shear failure of the underlying soil. $q_u$ on uniform soil with shear strength parameters cohesion (c) and friction angle ($\phi$) can be calculated using the conventional bearing capacity equation given in a general form (Eq. 1).

$$q_u = cN_cS_cd_cg_ci_cb_c + qN_qS_qd_qg_qi_qb_q + 0.5\gamma BN_\gamma S_\gamma d_\gamma g_\gamma i_\gamma b_\gamma \quad [1]$$

Where $N_{c,q,\gamma}$ are bearing capacity factors, $S_{c,q,\gamma}$ are shape factors, $d_{c,q,\gamma}$ are depth factors, $g_{c,q,\gamma}$ are ground slope factors, $i_{c,q,\gamma}$ are load inclination factors, $b_{c,q,\gamma}$ are base tilt factors, q is surrounding overburden pressure at foundation level, B is width or least plan dimension of foundation, c is soil cohesion, and $\gamma$ is effective unit weight of foundation soil.

The conventional bearing capacity equations by Hansen (1970) and Vesic (1973,1975) use ground slope modification factors which consider only footings at the crest of slope. On the other hand, Bowles (1997) proposed modified bearing capacity factors ($N'_c$, $N'_q$, $N'_\gamma$) which include depth and ground slope factors for footing placed on or adjacent to slope crest (Eq. 2). Bowles (1997) tabulated values of $N'_c$ & $N'_q$ & provided expression for $N'_\gamma$.

$$q_u = cN'_cS_{ci}i_c + qN'_qS_{qi}i_q + 0.5\gamma BN'_\gamma S_{\gamma i}i_\gamma \quad [2]$$

Researchers such as Keskin and Laman (2012), Castelli and Lentini (2012), Azzam and El Wakil (2015) and Acharyya and Dey (2017) carried out experimental and numerical tests to understand the failure mechanisms and study the effect of sloping ground on bearing capacity of footings.

## 2 NUMERICAL SIMULATIONS

### 2.1 Model Development

The commercial finite element software PLAXIS 3D (Version 20.0.0.119 © 2019) was used to conduct the numerical simulations. The typical PLAXIS model used for numerical simulations is depicted in Figure 1(a) & (b).

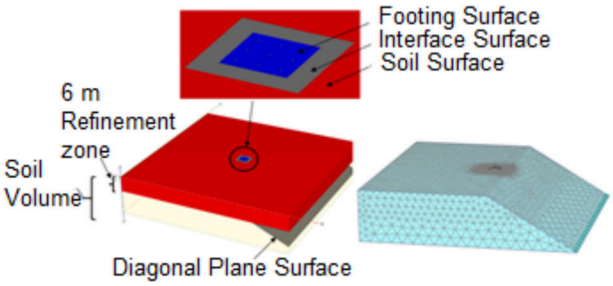


Figure 1. PLAXIS model used for numerical simulation of footings placed on ground surface with slope.

The finite element model was created in PLAXIS 3D by first defining a uniform subsurface soil volume with a single borehole as shown in Figure 1. Ground water level was considered near the bottom of the model to eliminate the effect of pore water pressure on the bearing capacity. Mohr-Coulomb constitutive model was chosen for soil in order to be consistent with the conventional bearing capacity analytical approach. The soil material properties including soil density, stiffness, Poisson's ratio and shear strength parameters were then defined. Non-associated flow rule was adopted with dilation angle (ψ) set to zero because it will cause more plastic volume change during failure, which is unrealistic for natural soils (Van Baars 2018). Tension cut-off was not also considered in the finite element models (Van Baars 2018).

The footing was modeled with plate as shown in Figure 1. The plate properties including plate thickness, density, elastic modulus and Poisson's ratio were then assigned. The footing plate properties resembled a typical concrete structure and considered to be as rigid as concrete, which is discussed later in Section 2.3. An interface surface was created underneath the footing plate and extended 1 m beyond the footing edge, as shown in Figure 1, to properly model the soil-structure interaction and abrupt change of footing pressure between the footing plate and surrounding soil. The interface was modeled with the same properties of adjacent soil without strength reduction for the interface.

The basic soil elements of the PLAXIS 3D finite element mesh are the 10-node tetrahedral elements. In addition, special types of elements are used to model structural behavior such as 6-node elements for plates and 12-node elements for interface surface. A global mesh was first generated for the entire volume of model. Mesh refining was then applied to the upper portion of soil volume (called "Refinement Zone" shown in Figure 1), to the footing plate, and to the interface surface. Mesh refining was enabled with the use of "coarseness factor" (CF) which is multiplied with the global element size.

Three calculation phases were considered in the "Staged Construction" mode of PLAXIS 3D. The first phase, called "Initial Phase", involved the generation of initial stress conditions for plane ground condition without footing load. The "Gravity Loading" option was used to generate the initial stress condition, because field equilibrium of the generated initial stresses is satisfied using this option. The second phase, called "Excavation Phase", involved the creation of sloping ground by deactivating a soil wedge formed by cutting the initial soil volume with a diagonal plane surface shown in Figure 1(a). For cohesionless soil, the ground slope was limited to the soil internal friction angle, (ϕ). For cohesive soil, the maximum allowable ground slope was determined with undrained slope stability analysis. A plastic calculation was run in the second phase to assess the amount of slope movement due to excavation. The third phase, called "Footing Load Phase", involved the application of footing load by activating the footing plate and prescribing uniform vertical displacement to represent rigid footing condition. The horizontal prescribed displacements were set to "fixed" to model a rough footing condition. All the displacements and small strains were reset to zero before moving to the second and third calculation phases.

The model was fixed in the normal directions at the vertical boundaries, fully fixed in all directions at the bottom boundary and free at the top model surfaces. In the "Numerical Control Parameters" options, the "Arc-length control type" was set to off and the "Desired maximum number of iterations" set to 60, both as necessary, because the default values couldn't allow to carryout large prescribed displacement analysis in some cases.

### 2.2 Numerical Simulation Program

A total of 258 numerical simulations of square footings placed on or near sloping ground surface of uniform soil were carried out in this research. 137 numerical simulations were carried out on drained cohesionless soils while the other 121 simulations on undrained cohesive soils as shown in Table 1. The square footings considered for the numerical simulations were 1mx1m and 3mx3m, which reflect the range of footing sizes in practice. The

numerical simulation study was carried out only for the case of footings on the ground surface without embedment. The slope angle (β) was varied from 10 to $35^0$ while the footing setback distance (b) from the slope crest was varied from 0 to 8 m depending on the simulation cases.

Table 1. Soil properties used in simulations

| Cohesionless Soil ($\phi$ \| $E_d$ \| v) | Cohesive Soil ($c_u$ \| $E_u$ \| v) |
|---|---|
| $27^0$ \| 10MPa \| 0.33 | 25kPa \| 5MPa \| 0.495 |
| $30^0$ \| 20MPa \| 0.33 | 50kPa \| 10MPa \| 0.495 |
| $33^0$ \| 30MPa \| 0.33 | 100kPa \| 20MPa \| 0.495 |
| $37^0$ \| 40MPa \| 0.33 | 200kPa \| 40MPa \| 0.495 |

$c_u$ is undrained cohesion, Ed & Eu are drained and undrained soil elastic modulus, and v is Poisson's ratio.

The internal friction angles and undrained cohesion values were chosen to cover the commonly encountered values in practice. The corresponding elastic modulus values were determined on the basis of available correlations in literature. The undrained elastic modulus for cohesive soil was estimated as 200 times the undrained cohesion (Bowles 1997). For cohesionless soil, SPT number (N) was first estimated from correlation with the friction angle, and then the drained elastic modulus was estimated as 1200 N (Bowles 1997; Mineneh & Gilmour 2020).

## 2.3 Sensitivity Analysis

After setup of PLAXIS 3D model, sensitivity analysis was carried out to assess the effect of different parameters. The parameters that may affect the PLAXIS model results are model parameters (model dimensions & mesh sizes), footing parameters (density, thickness, Young's modulus, Poisson's ratio), and soil parameters (internal friction angle, cohesion, Young's modulus, Poisson's ratio, unit weight, strength reduction factor - $R_{inter}$).

Sensitivity analysis was not performed for model size, and most of footing and soil parameters for the reasons discussed below.

Boundary effects on bearing capacities are negligible for offset distances from footing edge of about 2 to 3 times footing width laterally and about 4 times footing width vertically (Bowles 1997). In the PLAXIS simulations for 1mx1m and 3mx3m footings, a model size of 63mx63mx15m (6m Refinement Zone) was used which has minimum offset distance of 10 times footing width laterally and 5 times footing width vertically.

For 1mx1m footing size, few simulations were also conducted using a model size of 21mx21mx5m (2m Refinement Zone) which will reduce the mesh sizes while keeping fairly similar number of meshes as the larger model size. The smaller model size for 1mx1m footing lowered the measured bearing capacities by about 10%.

A typical rigid, reinforced concrete footing has Young's modulus of about 30 GPa, and Poisson's ratio of about 0.15. These typical values were used in the numerical simulations as they don't vary significantly in practice.

The footing load was applied by prescribing a uniform displacement on the footing plate to ensure rigidity of the footing. Thus, the effect of footing thickness will be eliminated as the footing plate will behave as rigid regardless of its thickness. In addition, a largest practical footing thickness of 1 m was used to further enforce rigid behavior.

Poisson's Ratio (v) of 0.495 was considered for cohesive soil to model undrained condition. A v value of 0.33 was used for all cohesionless soil since its variation will not have significant effect on bearing capacity values. Unit weight of 20 kN/$m^3$ was considered for all soil types and simulations as it will not vary significantly.

The interface surface between the footing plate and soil was introduced to properly model the soil-structure interaction and abrupt change of footing load from plate to adjacent soil. Since finest surface mesh is desired for such modeling, the smallest possible mesh coarseness factor (CF) of less than 0.035 was used for the interface surface. The interface surface was also modeled with similar properties of the soil by setting the $R_{inter}$ value to 1.

### 2.3.1 Sensitivity for Cohesionless Soil

Sensitivity analysis was completed for mesh sizes and selected input parameters as presented below.

#### 2.3.1.1 Global Mesh Size

Five options of global mesh sizes are available in PLAXIS 3D, namely Very Fine, Fine, Medium, Coarse and Very Coarse. The coarse mesh sizes were not considered as the simulation results may not be accurate even though the analyses would take less computation time. In order to determine optimum global mesh size, sensitivity analysis was carried out for 1mx1m and 3mx3m footing sizes to compare Fine and Medium mesh sizes keeping other inputs similar.

Less than 5% difference of ultimate capacity was observed between Fine and Medium global mesh sizes. Thus, a Fine global mesh size was considered for the simulations in this research. Further refining of mesh size was investigated for the upper portion of soil using mesh Refinement Zone (Figure 1) as discussed below.

#### 2.3.1.2 Mesh Refinement Zone

A mesh Refinement Zone was introduced for the upper portion of soil layer, as shown in Figure 1, to get flexibility to refine the mesh sizes within the wedge shear failure zone of the soil. The mesh size of the Refinement Zone was modified using its coarseness factor (CF) which is a multiplier to the global element size. A CF of less than unity will decrease the local mesh size from the global.

Other inputs being the same, simulations were carried out for Refinement Zone CF values varied between 1 & 0.3 for 3mx3m footing size. Similar load-deformation curves were obtained despite the variation of CF values. A reasonable Refinement Zone CF value of 0.7 was selected for the simulations of 3mx3m footings.

Sensitivity analysis was also carried out for 1mx1m footing by varying the Refinement Zone CF between 0.3

and 1, and no effect was observed on the load-deformation curves. Thus, appropriate CF values within the above range were used to complete the simulations in reasonable computational time.

#### 2.3.1.3 Plate Mesh Size

The effect of footing plate mesh size on numerical results was investigated by varying the plate CF between 0.1 & 0.04 for footing sizes of 3mx3m. It should be noted that the smallest possible CF value in PLAXIS3D was 0.03125.

Minor differences in bearing capacity of 5% for 3mx3m footing was obtained. Thus, the smaller plate CF values of 0.04 to 0.045 were considered for the numerical simulations in this research.

#### 2.3.1.4 Interface Surface Mesh size

Since the interface surface was required for proper modeling of the soil-footing interaction and abrupt change of footing pressure, finest mesh is desired for the interface surface. Thus, the smallest coarseness factor (CF) of less than 0.035 was assigned to the interface surface of the numerical simulations in this research.

However, some sensitivity tests were carried out to understand the effect of interface surface mesh size on the bearing capacity results. It was concluded from the sensitivity test results that the interface surface mesh size would affect the numerical result if it is finer than the plate mesh size. This finding supports the necessity of interface surface finest than the footing plate and soil.

#### 2.3.1.5 Soil Elastic Modulus and Footing Unit Weight

Sensitivity analysis was carried out for different values of soil elastic modulus to investigate its influence on the numerical results. The results show that the soil modulus influences the load-deformation curves, but the ultimate load capacity appears to be the same regardless of soil modulus value.

Sensitivity analysis was also carried out for different values of soil unit weight to investigate its influence on the numerical results. The results show that the bearing capacity of tests with no footing weight are higher than the tests with footing weight by the amount equal to the weight of the footing. Thus, the footing weight will reduce the measured bearing capacity by the amount equal to its weight. For simplicity, no footing weight was considered in the numerical simulations of this research.

### 2.3.2 Sensitivity for Cohesive Soil

Sensitivity analysis was also completed for mesh sizes and soil elastic modulus in cohesive soil.

Global mesh sizes determined for cohesionless soil in Section 2.3.1.1 were also used for cohesive soil.

Sensitivity analysis of refinement zone mesh sizes for cohesive soil was carried out by varying the Refinement Zone CF between 0.2 and 1 for cases of 1mx1m and 3mx3m footing sizes. The load-deformation curves obtained from all analyses within each footing size appear to be similar. Thus, similar refinement zone mesh sizes as the cohesionless soil, Section 2.3.1.2, were used.

The plate coarseness factor (CF) was varied between 0.04 and 0.1 for 3mx3m footing, which resulted in similar bearing capacity. Thus, the smaller plate CF values of 0.04 to 0.045 were used as indicated in Section 2.3.1.3.

Sensitivity analysis was carried out for different elastic modulus of cohesive soil for both 3mx3m and 1mx1m footing sizes. Similar result was obtained as discussed in Section 2.3.1.5.

## 2.4 Model Validation and Calibration

To validate the numerical model, the bearing capacity values determined from the simulations were compared with the conventional bearing capacity equations of Terzaghi (1943) and Meyerhof (1963). The limited available small-scale footing experiments could not be used for validation or calibration because of a scale effect.

The ultimate capacity in the simulations was taken from the load-deformation curves when the load approaches to an asymptote value at large deformation mostly after 0.2 to 0.3B.

The conventional bearing capacity equations are given in Eq. 3 for cohesionless soil and in Eq. 4 for cohesive soils.

$$q_u = \tfrac{1}{2}\,\gamma\, B\, N_\gamma\, S_\gamma \qquad [3]$$

$$q_u = c_u\, N_c\, S_c \qquad [4]$$

$S_\gamma$ was 0.8 for Terzaghi (1943). $N_c$ was 5.7 for Terzaghi (1943) and 5.14 for Meyerhof (1963). $S_c$ was 1.3 for Terzaghi (1943) and 1.2 for Meyerhof (1963). The original papers can be referenced for expressions of $N_\gamma$ and Meyerhof's $S_\gamma$.

The bearing capacity values obtained from the simulations are compared with the values calculated by Terzaghi and Meyerhof equations in Figure 2 for cohesionless soil and in Figure 3 for cohesive soil.

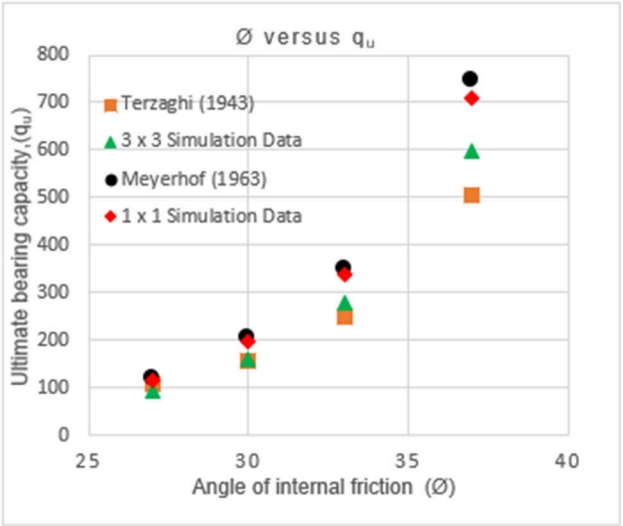


Figure 2. Comparison between numerical and analytical bearing capacities for cohesionless soil.

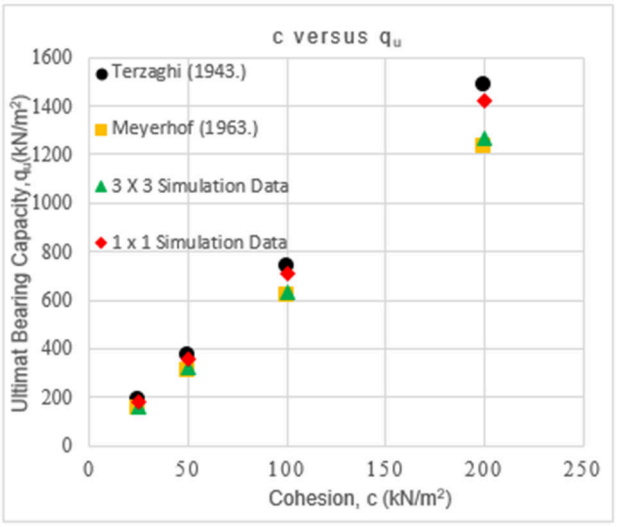


Figure 3. Comparison between numerical and analytical bearing capacities for cohesive soil.

The conventional equations generally predict the simulation results at lower shear strength values and scatter slightly with the increase of strength parameter values. Meyerhof is the upper bound solution while Terzaghi is the lower bound solution for cohesionless soil, and vice versa for cohesive soil.

## 2.5 Stability of Ground Slopes

The numerical simulations to study footing bearing capacity were carried out on stable ground slopes against global slope failure. For cohesionless soil, the slope angle (β) was varied equal or less than the angle of repose which is equal to the soil internal angle of friction (ϕ). For cohesive soil, slope stability analysis was carried out to determine the maximum possible slope angle and height based on Taylor's slope stability chart method (Braja M. Das, 2010).

For the case of $c_u$ = 25 kPa, a maximum slope angle of 53 degree can be achieved with a maximum slope height of 7m. Thus, for numerical simulations using cohesion of 25 kPa, conservative slope angles of not more than 30 degree and slope height of 7 m were considered. Also, the shear failure was examined not to extend below 7 m depth to ensure the full slope effect on the bearing capacity was considered.

For $c_u$ = 50 kPa, a maximum slope angle of 50 degree can be achieved with a maximum slope height of 13.9m. Thus, for numerical simulations using cohesion of 50 kPa, conservative slope angles of not more than 30 degree were considered for slope height of 15 m. For cohesions of 100 kPa and 200 kPa, slope stability analysis was not needed as maximum slope angle of 35 degree and slope height of 15 m were considered in the numerical simulations.

To confirm the Taylor's chart analysis, slope stability analysis was also carried out using limit equilibrium method using the above geometries for undrained cohesion of 25 kPa and 50 kPa.

# 3 RESULTS AND DISCUSSIONS

## 3.1 Evaluation of Existing Bearing Capacity Equations

### 3.1.1 Hansen (1970) and Vesic (1975)

Hansen (1970) and Vesic (1975) bearing capacity equations with ground modification factors were evaluated with the numerical simulation data in this paper.

#### 3.1.1.1 Cohesionless soil

As shown in Figure 4, there is a minor difference between Hansen and Vesic predictions. However, both methods significantly underpredict the bearing capacity compared to the present research for footings at the crest of a slope. The theoretical prediction of ground modification factor is lower than the simulation data at fairly constant value of 0.25 to 0.3. Thus, the theoretical modification factors provided by Hansen and Vesic can be improved by adding an average constant term of 0.275. Also, ground modification factor determined from the simulation data appears to be fairly independent of the soil friction angle and footing size for the case of no setback distance. This observation confirms the theoretical ground modification factors of Hansen and Vesic which depend only on the slope angle and not the soil friction angle.

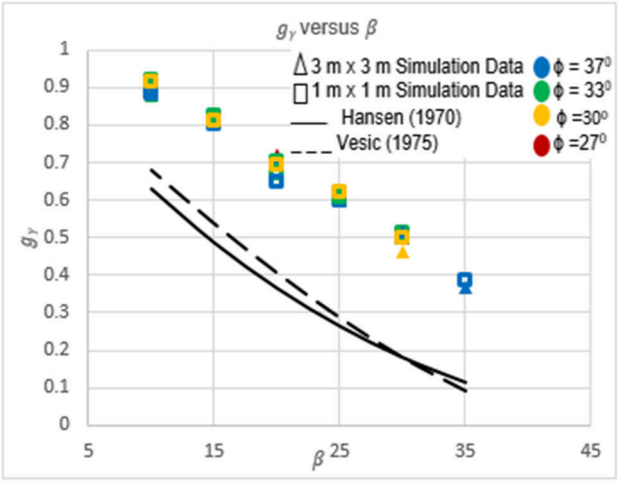


Figure 4. Ground modification factor ($g_\gamma$) versus Slope Angle (β)

#### 3.1.1.2 Cohesive Soil

A ground modification factor for the cohesion term was not obtained from Hansen (1970) publication. Thus, only Vesic (1975) was used to predict the simulation data as shown in Figure 5. The numerical simulation data in Figure 5 do not show significant effect of ground slopes on bearing capacity with the maximum reduction of bearing capacity being only 11% for slope angle of $35^0$ and $c_u$ of 200 kPa. Vesic ground factor was generally lower than the simulation data and increases with slope angle.

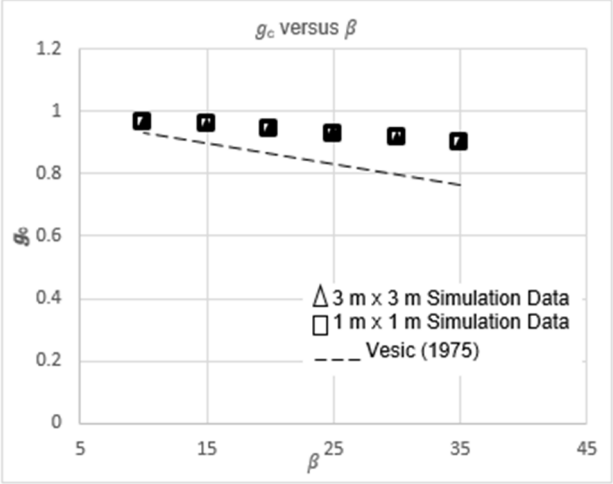


Figure 5. Ground modification factor ($g_c$) versus Slope angle (β). The data points overlap for cohesions of 25kPa, 50kPa, 100kPa and 200kPa. For slope angle of $35^0$, simulations were conducted only for cohesion of 200kPa.

3.1.2 Bowles (1997)

Bowles (1997) bearing capacity equation with modification of bearing capacity factors is evaluated with the numerical simulation data in this research.

3.1.2.1 Cohesionless Soil

The numerical simulation data and predictions of Bowles (1997) equation for cohesionless soil are presented in Figures 7 to 10. The ground modification factor ($g_\gamma$) calculated from Bowles equation varies linearly from a smallest value at zero setback distance to a value of 1 at setback distance of twice the footing width. The reduction factor converges to 1 regardless of slope angle and internal friction angle. On the other hand, the ground modification factor ($g_\gamma$) determined from the numerical simulation data generally varies in hyperbolic trend instead of linear trend. Thus, Bowles approach doesn't predict the general trend of the variation of the ground factor as well as provides significantly low values of ground factor or bearing capacity on slope. The only exception is when the measured ground factor from the simulation data falls below 0.5 for high slope angles such as $35^0$ as shown in Figure 10. Based on Bowles prediction of individual simulation data, it estimated the bearing capacity on slope -32 to +26 % of the simulation data.

3.1.2.2 Cohesive Soil

The numerical simulation data and predictions of Bowles (1997) equation for cohesive soil are presented in Figures 12 to 15. Similar to the case of cohesionless soil, Bowles prediction of the ground modification factor for cohesive soil varies linearly from a smallest value at zero setback distance to a value of 1 at setback distance of about 0.75 times the footing width. It converges to 1 regardless of slope angle and undrained cohesion. On the other hand, the ground modification factor determined from the numerical simulation data generally varies in hyperbolic trend. The numerical data also show the convergence of the reduction factor to 1 at about 0.75 times the footing width. Bowles approach resulted in significantly lower values of ground factor and bearing capacity on slope. Bowles estimated the bearing capacity on slope by average of -10 % of the simulation data.

3.2 Proposed Model

New ground modification factors $g_\gamma^A$ and $g_c^A$ are proposed for the friction and cohesion terms of the conventional bearing capacity equation, respectively, based on the numerical simulation data presented in this paper.

3.2.1 Proposed Ground Modification Factor for Cohesionless Soil ($g_\gamma^A$)

The newly proposed ground modification factor was determined by best fitting the data points with a surface of polynomial function. The numerical data points and the best fit surface are shown in Figure 6. The best-fit surface was obtained with regression analysis using MATLAB version 9.1 (R2016b). In MATLAB, curve fitting toolbox provides an app and functions for fitting curves and surfaces to data. One can create a Polynomial surface of up to degree five (5). Also, the custom equation window allows users to specify surface fitting equations for nonlinear regression. In this research, the simulation data were processed in terms of b/B, $R_\gamma$, and $g_\gamma$ (as defined in next paragraphs), and the surface is fitted interactively by loading the excel data at the MATLAB command line. $g_\gamma$ is selected as a dependent variable while b/B and $R_\gamma$ are selected as independent variables in the curve fitting app. Then, different model types were evaluated using the fit category drop-down list. A best fit surface with high coefficient of correlation is obtained using a polynomial equation to the power of two (2) as given in Eq. 5 below.

$$g_\gamma^A = 0.3755 + (0.5512 \times b/B) + (1.876 \times R_\gamma) - (0.6976 \times b/B \times R_\gamma) - (0.1238 \times (b/B)^2) - (1.619 \times R_\gamma^2) \quad [5]$$

For b/B ratio $\geq 2$, $g_\gamma^A = 1$

$R^2 = 0.9384$, Where $R^2$ is the coefficient of determination

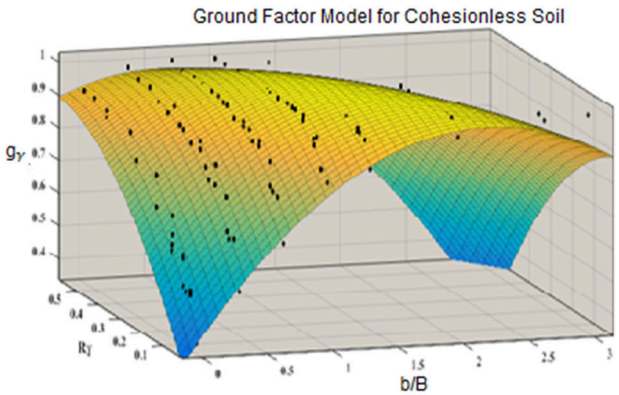


Figure 6. Data points and best fit surface for cohesionless soil.

The b/B ratio refers to the ratio of setback distance (b) between slope crest and footing outside edge to the footing width (B). The ground modification factor ($g_\gamma$) refers to the ratio of footing capacity on slope (Fs) to footing capacity on plane ground (Fp).

The presence of slope boundary near footing results in a partial development of the passive zone, thus resulting in a reduced bearing capacity. In this paper, the reduction in passive resistance due to the presence of slope is computed following Bowles (1997) approach, which relates the resistance reduction to the ratio "$R_\gamma$" of minimum passive pressure coefficient ($K_{min}$) to maximum passive pressure coefficient ($K_{max}$). The pressure coefficients are computed using Coulomb passive pressure theory and considering β = (-) for $K_{min}$, β = (0) for $K_{max}$, and ϕ=δ for both $K_{min}$ and $K_{max}$. The ratio "$R_\gamma$" considers the effects of both the soil internal friction angle (ϕ) and slope angle (β).

3.2.1.1 Evaluation of Proposed Ground Factor ($g_\gamma^A$) with Simulation Data

The bearing capacity reduction factors due to slope (which are equivalent to the ground factors) obtained from the numerical simulations were compared with the predictions of the proposed model in Eq. 5 as presented in Figures 7 to 10.

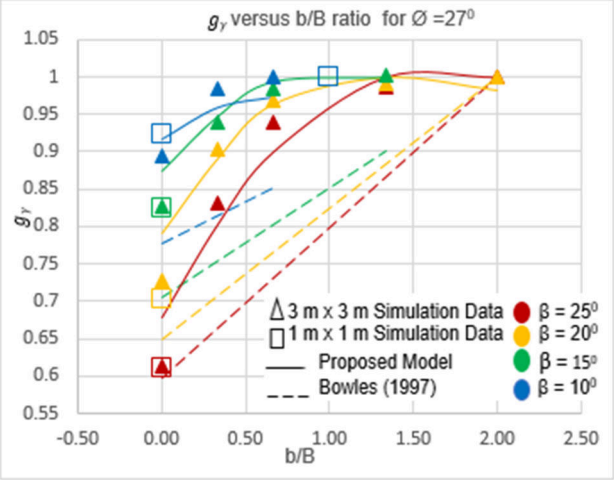


Figure 7. $g_\gamma$ versus b/B for ϕ of $27^0$

It can be noted from the above figures that good agreement between the proposed model and simulation data for the ground factor ($g_\gamma$) was achieved both in terms of the trend and actual values. At some data points, larger error of up to ±19% was encountered; however, the average error does not exceed ±10 % for both 1m x 1m and 3m x 3m footing size. The proposed model is a convergent function. As the setback distance from slope crest increases, the influence of slope diminishes, and in general at b/B=2, the slope face imposes no further influence and the proposed model approaches to unity. The proposed model improves Bowles approach using non-linear equation.

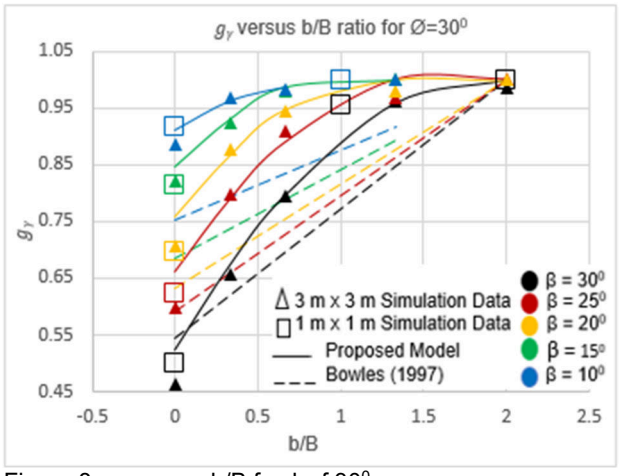


Figure 8. $g_\gamma$ versus b/B for ϕ of $30^0$

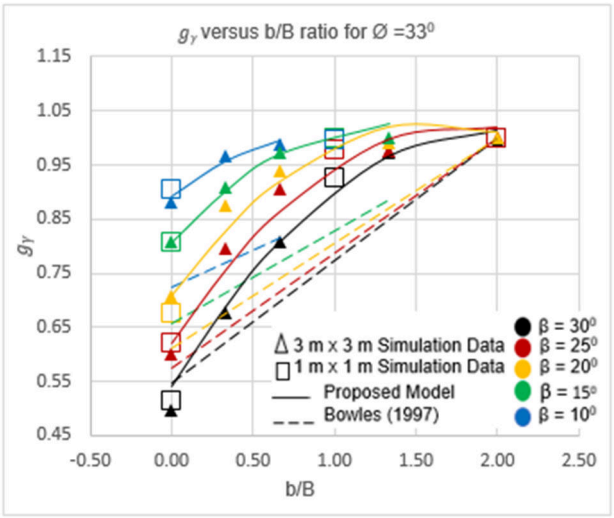


Figure 9. $g_\gamma$ versus b/B for ϕ of $33^0$

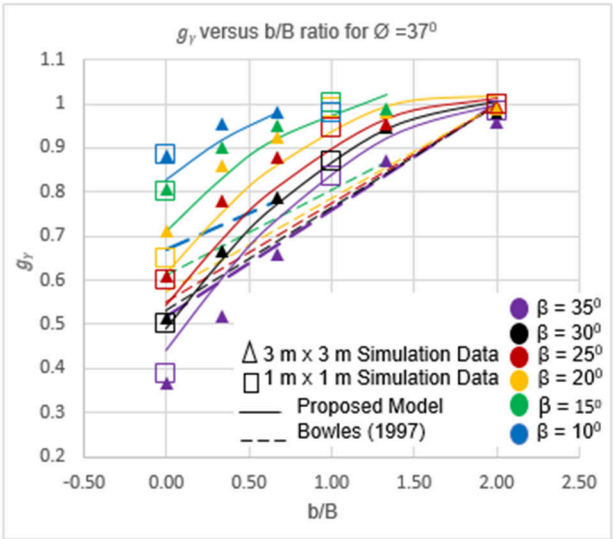


Figure 10. $g_\gamma$ versus b/B for ϕ of $37^0$

### 3.2.2 Proposed Ground Modification Factor for Cohesive Soil ($g_c^A$)

In similar approach to the cohesionless soil, a new ground modification factor for cohesive soil was determined by best fitting the data points with a surface of polynomial function using MATLAB. The numerical data points and the best fit surface are shown in Figure 11. A best-fit surface with a high coefficient of correlation is obtained using a polynomial equation to the power of three (3) as given in Eq. 6 below.

$$g_c^A = 0.9914 + (0.1055 \times b/B) - (0.1364 \times R_c) + (0.2289 \times b/B \times R_c) - (0.1671 \times (b/B)^2) - (0.08003 \times (b/B)^2 \times R_c) + (0.05823 \times (b/B)^3 \quad [6]$$

For b/B ratio ≥ 0.75, $g_c^A = 1$

$R^2 = 0.9328$, Where $R^2$ is the coefficient of determination

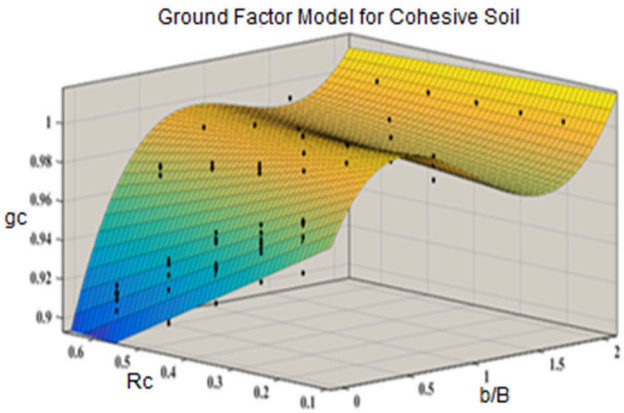


Figure 11. Data points and best fit surface for cohesive soil

For cohesive soil in undrained condition, both $K_{min}$ and $K_{max}$ (defined in the previous section) will be 1 for slope angles β = (-) or (0). Thus, the reduction of passive resistance in cohesive soil due to the presence of slope "Rc" is considered to be a function of tanβ which is proportional to the loss of soil mass (overburden pressure) due to the presence of slope.

#### 3.2.2.1 Evaluation of Proposed Ground Factor ($g_c^A$) with Simulation Data

The bearing capacity reduction factors due to slope (which are equivalent to the ground factors) obtained from the numerical simulations of cohesive soil were compared with the predictions of the proposed model in Eq. 6 as presented in Figures 12 to 15.

As observed in the figures, the proposed ground modification model predicts both the hyperbolic trend and the data values of the bearing capacity reduction factors (ground modification factors) obtained from the numerical simulations. It is also observed that the ground factors from the numerical simulation converge to unity at b/B values in the range of 0.75 to 1.

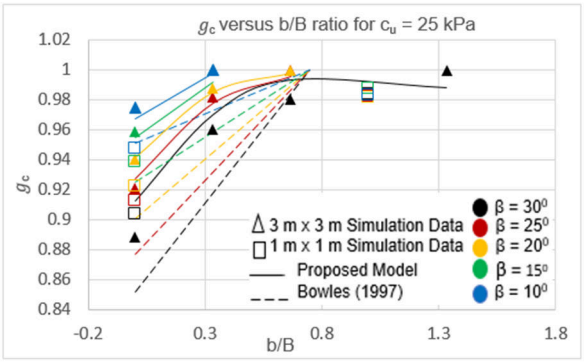


Figure 12. $g_c$ versus b/B for $c_u$ of 25 kPa

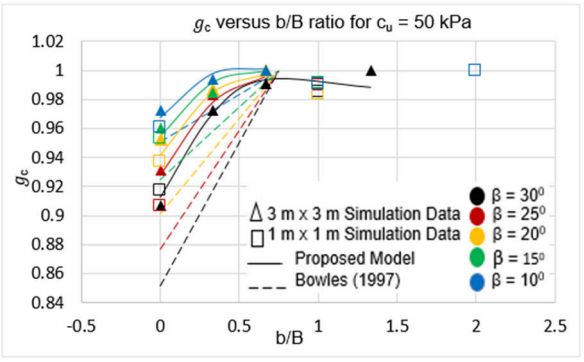


Figure 13. $g_c$ versus b/B for $c_u$ of 50 kPa

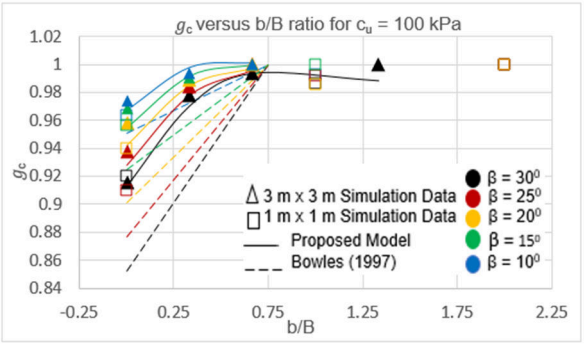


Figure 14. $g_c$ versus b/B for $c_u$ of 100 kPa

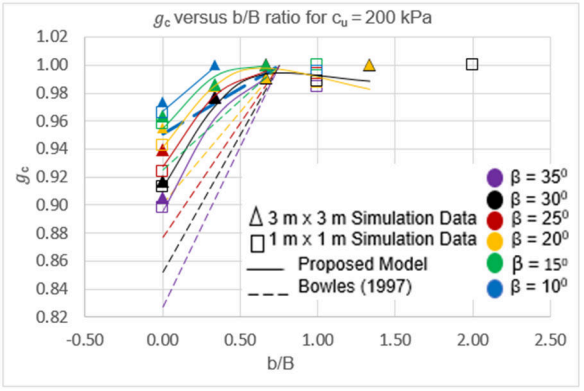


Figure 15. $g_c$ versus b/B for $c_u$ of 200 kPa

### 3.3 Failure Mechanism and Stress Distribution

Examples of slope effect on the failure mechanism are presented in Figures 16.

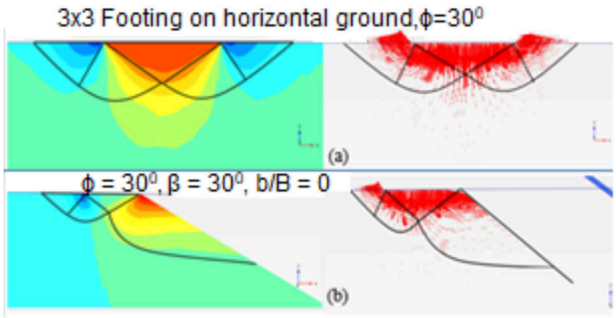


Figure 16. Example of formation of passive zones.

The typical contact pressure distributions for rigid footings on cohesionless and cohesive soils are also observed in the simulations as shown in Figures 17 & 18.

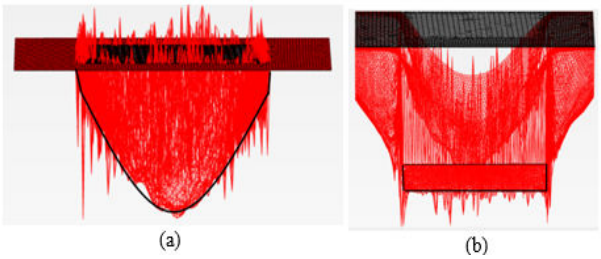


Figure 17. (a) Stress distribution, (b) Footing deformation beneath a rigid footing on cohesionless soil

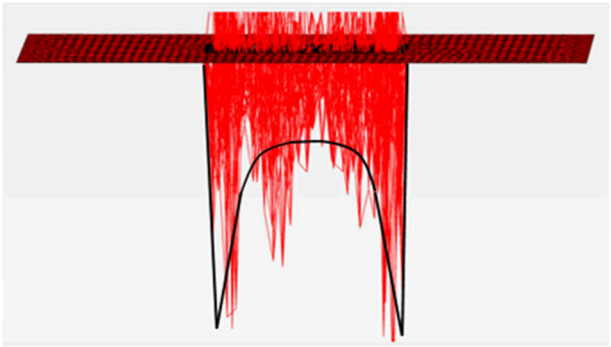

Figure 18. Stress distribution beneath a rigid footing on cohesive soil

## 4 CONCLUSIONS AND RECOMMENDATIONS

For cohesionless soil, Hansen (1970) and Vesic (1975) equations significantly underpredict the bearing capacity of footings placed at crest of slope. The ground modification factors provided by Hansen (1970) and Vesic (1975) can be improved by adding an average constant term of 0.275. For cohesive soil, Vesic (1975) equation slightly underestimates the bearing capacity.

Bowles (1997) approach enables to calculate bearing capacity for footings with setback distance of greater than zero from slope crest. However, Bowles approach doesn't predict the general trend of the variation of ground factor with setback distance as well as provides significantly low or high values of ground factor or bearing capacity.

Improved ground modification factors are proposed which consider shear strength parameters, set back distance, footing size and slope angle. These modification factors can be implemented in the general bearing capacity equation.

The improved ground modification factors generally vary in hyperbolic trend with setback distance. They converge to unity beyond a critical set back ratio (b/B) of 2 for cohesionless soil and around 0.75 for cohesive soil, which are in agreement with Bowles (1997) approach.

## 5 REFERENCES


Acharyya, R., & Dey, A. 2017. Finite Element Investigation of the Bearing Capacity of Square Footings Resting on Sloping Ground. Indian National Academy of Engineering.

Azzam, W., & El Wakil, A. Z. 2015. Experimental and Numerical Studies of Circular Footing Resting on Confined Granular Subgrade Adjacent to Slope. International Journal of Geomechanics.

Bowles, J. E. 1997. Foundation Analysis and Design. New York: The McGraw-Hill Companies, Inc.

Castelli, F., & Lentini, V. 2012. Evaluation of the bearing capacity of footings on slopes. International Journal of physical modelling in geotechnics, 112-118.

Das, Braja M. 2010. *Principles of Geotechnical Engineering*, 7th ed.,: Cengage Learning, Massachusetts, USA.

Hansen. 1970. A Revised and Extended Formula for bearing capacity. The Danish Geotechnical Institute, Bulletin No. 28, (pp. 3-21). Copenhagen.

Keskin, M., & Laman, M. 2012. Model Studies of Bearing Capacity of Strip Footing on Sand Slope. KSCE Journal of Civil Engineering (2013) 17(4):699-711, 699-711.

Meyerhof., G. G. 1963. Some recent research on the bearing capacity of foundations. Canadian Geotechnical Journal, vol. I, no.1, 16-26.

Terzaghi., K. 1943. Theoretical Soil Mechanics. New York: John Wiley and Sons, Inc.

Van Baars, Stefan. 2018. Numerical check of the Meyerhof bearing Capacity equation for shallow foundations. Innovative Infrastructure solutions, 3.10.1007/s41062-017-0116-1.

Vesic, A. S. 1975. Bearing Capacity of Shallow Foundations. In H. F. Winterkorn, & H.-y. Fang, Foundation Engineering Handbook (pp. 121-145). Durham: New York Van Nostrand Reinhold.

Vesic., A. S. 1973. Analysis of Ultimate Loads of Shallow Foundations. Journal of the soil Mechanics and foundations division, 45-71.